



Cite this: *Org. Biomol. Chem.*, 2015, **13**, 2974

## Hybridization of an A $\beta$ -specific antibody fragment with aminopyrazole-based $\beta$ -sheet ligands displays striking enhancement of target affinity<sup>†</sup>

Marco Hellmert,<sup>a</sup> Andreas Müller-Schiffmann,<sup>b</sup> Max Sena Peters,<sup>a</sup> Carsten Korth<sup>\*b</sup> and Thomas Schrader<sup>\*a</sup>

Determining A $\beta$  levels in body fluids remains a powerful tool in the diagnostics of Alzheimer's disease. This report delineates a new supramolecular strategy which increases the affinity of antibodies towards A $\beta$  to make diagnostic procedures more sensitive. A monoclonal antibody IC16 was generated to an N-terminal epitope of A $\beta$  and the variable regions of the heavy and light chains were cloned as a recombinant protein (scFv). A 6  $\times$  histidine tag was fused to the C-terminus of IC16-scFv allowing hybridization with a small organic  $\beta$ -sheet binder via Ni-NTA complexation. On the other hand, a multivalent nitrilotriacetic acid (NTA)-equipped trimeric aminopyrazole (AP) derivative was synthesized based on a cyclam platform; and experimental evidence was obtained for efficient Ni<sup>2+</sup>-mediated complex formation with the histidine-tagged antibody species. In a proof of principle experiment the hybrid molecule showed a strong increase in affinity towards A $\beta$ . Thus, the specific binding power of recombinant antibody fragments to their  $\beta$ -sheet rich targets can be conveniently enhanced by non-covalent hybridization with small organic  $\beta$ -sheet binders.

Received 15th November 2014,  
Accepted 13th January 2015

DOI: 10.1039/c4ob02411g

[www.rsc.org/obc](http://www.rsc.org/obc)

## Introduction

Alzheimer's disease (AD) is a progressive neurodegenerative disease, that is neuropathologically characterized by extracellular deposits of amyloid plaques consisting of amyloid-beta (A $\beta$ ) peptides and intracellular accumulation of hyperphosphorylated microtubule associated protein tau. The aggregation of A $\beta$  and tau leads to neuronal loss and ultimately to severe dementia and death. To date no cure is available and recently several promising treatment options failed, most likely because drug administration comes too late. Therefore, early diagnosis of AD is not only important for medication of initial symptoms but will also be required for potential future therapeutic interventions.

A $\beta$  refers to peptides of 39-43 amino acids emerging from the amyloid precursor protein (APP) through proteolytic cleavage.<sup>1</sup> One of these, *i.e.*, A $\beta$ (1-42), plays a central role in the pathogenesis of Alzheimer's disease (AD)<sup>2,3</sup> since it aggregates into highly neurotoxic oligomers, which ultimately form

amyloid fibrils. Similarly, the tau protein self-assembles, after hyperphosphorylation, into highly toxic neurofibrillary tangles.<sup>4</sup> Although other proteins are discussed as the major cause for related protein misfolding diseases, A $\beta$ (1-42) also seems to play a certain role in Parkinson's disease and Huntington's chorea<sup>5</sup> as well as in the context of diabetes mellitus type 2 and Down syndrome.<sup>6,7</sup>

Whereas monomeric A $\beta$  is present at a physiologically normal metabolism and supposedly has an antimicrobial function,<sup>8,9</sup> its oligomeric forms are highly neurotoxic and considered one of the major factors in the development of AD.<sup>2</sup> Initially, levels of the aggregation prone A $\beta$ (1-42) peptide are elevated either by increased production or decreased clearance, which leads to formation of synaptotoxic low-*n* oligomeric A $\beta$  species, like dimers and trimers.

These oligomers adopt a  $\beta$ -sheet-rich tertiary structure and form insoluble fibrillar aggregates, which deposit outside neurons as amyloid plaques.<sup>10</sup> Increase of  $\beta$ -sheet rich small soluble A $\beta$  oligomers and insoluble A $\beta$  is strongly correlated to the progress of disease and therefore displays a prime target for diagnostic agents. However, early detection of low picomolar concentrations of A $\beta$  oligomers in body fluids (blood serum, cerebrospinal fluid) is challenging, and reaches the limit of antibody sensitivities. Therefore it is highly desirable to enhance the affinity of A $\beta$  specific antibodies.

In recent years our group has developed trimeric aminopyrazole (AP) based  $\beta$ -sheet ligands by rational design. These

<sup>a</sup>Institute for Organic Chemistry, University of Duisburg-Essen, Universitätsstr. 7, 45117 Essen, Germany. E-mail: thomas.schrader@uni-due.de

<sup>b</sup>Department of Neuropathology, Heinrich Heine University, Moorenstr. 5, 40225 Düsseldorf, Germany. E-mail: ckorth@uni-duesseldorf.de

<sup>†</sup>Electronic supplementary information (ESI) available: Copies of the <sup>1</sup>H NMR and <sup>13</sup>C NMR spectra for all key intermediates and final products. See DOI: 10.1039/c4ob02411g



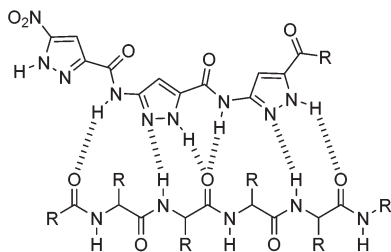


Fig. 1 Hydrogen-bond interactions between the trimeric aminopyrazole ligand ( $\text{DAD}$ )<sub>3</sub> with the peptide backbone of a  $\beta$ -strand ( $\text{ADA}$ )<sub>n</sub>.

contain a DAD order of hydrogen-bond donors and acceptors which perfectly matches the  $\beta$ -sheet structure formed by  $\text{A}\beta$  oligomers (Fig. 1). Most likely these agents bind to the KLVFF sequence of mono- and oligomeric  $\text{A}\beta$ .<sup>11–13</sup>

Meanwhile, we have synthesized a large variety of trimeric aminopyrazole derivatives with different C-terminal extensions and identified the most potent  $\beta$ -sheet breakers; their affinities towards  $\text{A}\beta$ , however remained moderate – in the low micromolar range.<sup>14</sup> In order to enhance *in vivo* efficiency we joined forces with the Willbold group and developed hybrid molecules consisting of the established  $\beta$ -sheet breaking AP-trimer covalently connected to polypeptides identified by phage display as effective selectors for  $\text{A}\beta$  oligomers.<sup>15</sup> These new hybrids displayed striking synergistic effects in cells where they completely suppressed  $\text{A}\beta$  oligomer formation as well as restored long term potentiation (LTP). As a logical extension, we decided to connect the aminopyrazole unit to  $\text{A}\beta$ -specific antibodies.

Much effort has lately been devoted to AD immunotherapy.<sup>16,17</sup> Most recently instead of large immunoglobulins, single-chain variable fragments (scFvs) have been utilized for  $\text{A}\beta$ -recognition, with the advantage of enhanced permeability through the blood-brain barrier accompanied by decreased *in vivo* side effects. Here, we employed a scFv-construct derived from an  $\text{A}\beta$  binding immunoglobulin (IC16) which targets the N-terminal domain (aa 2-8) of monomeric and aggregated  $\text{A}\beta$ <sup>18</sup> and combined it with the aminopyrazole trimer by non-covalent complexation. To this end the antibody species was equipped with a histidine tag at its C-terminus while the aminopyrazole was covalently linked to a trivalent nitriloacetic acid (NTA) moiety, allowing a highly stable  $\text{Ni}^{2+}$ -mediated complexation of the scFv with the aminopyrazole (Fig. 2). Although the 1:1 complex depicted in Fig. 2 agrees with modeling studies, one cannot exclude *a priori* the alternative formation of an overlapping 2:1 complex, in the form of (1-8 amyloid-1) – (IC16-scFv : AP-Ni-NTA-cyclam) – (16-20 amyloid-2).

We observed that this hybridization of two  $\text{A}\beta$  ligands greatly improved their affinity towards  $\text{A}\beta$ -peptides, providing the basis for new sensitive tools for diagnostic issues. Our results constitute a proof of principle for the general concept, that molecular recognition of  $\beta$ -sheet rich proteins by specific recombinant antibody fragments may be greatly enhanced through combination with small organic  $\beta$ -sheet binders. This

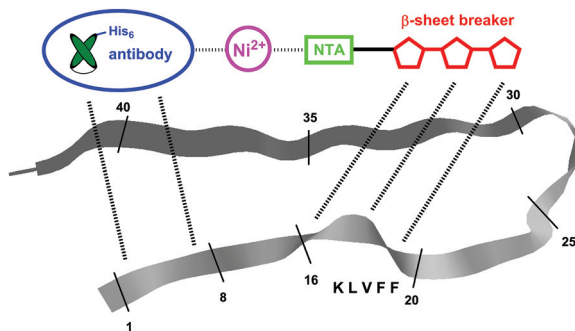


Fig. 2 Schematic representation of the  $\text{Ni}^{2+}$ -mediated His<sub>6</sub>-antibody/NTA-aminopyrazole hybrid targeting two different recognition sites on the  $\text{A}\beta$  monomer (aa 1-8 and the KLVFF sequence 16-20).

concept may be generally applicable to other proteins involved in neurodegenerative diseases.

## Results and discussion

In initial attempts with only one NTA head fused to the aminopyrazole trimer the formation of the desired AP-NTA- $\text{Ni}^{2+}$ -His<sub>6</sub>-antibody complex could not be confirmed. Consequently we aimed for an analogous multivalent complex with several NTA moieties placed on a suitable platform and connected to the aminopyrazole. In the ideal case, all six histidine moieties of the C-terminal tag should be addressed simultaneously. In their seminal work, Piehler *et al.* developed and optimized different scaffolds and indeed achieved greatly improved affinities towards histidine tags.<sup>19</sup> The most promising candidate consisted of a central cyclam unit equipped with three NTA groups leaving one free amine for further functionalization; this was in our case used as the attachment point for the aminopyrazole trimer. Compared to monovalent NTA units, the tris-NTA cyclam moiety displayed an increase in thermodynamic stability of 3 orders of magnitude, from 10  $\mu\text{M}$  to 10 nM affinity, accompanied with extremely slow dissociation kinetics. Fig. 3 shows our application for antibody-aminopyrazole hybridization and a proposed model of the octahedral  $\text{Ni}^{2+}$ -mediated NTA-histidine complexation.

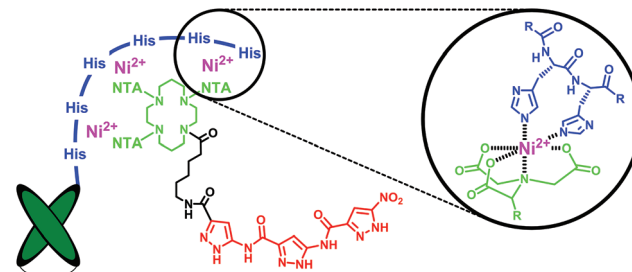


Fig. 3 Left: schematic representation of the proposed very tight complex between the His<sub>6</sub>-tagged antibody and the AP-cyclam-tris(NTA) moiety, mediated by  $\text{Ni}^{2+}$  ions. Right: proposed model of the NTA- $\text{Ni}^{2+}$ -histidine complexation.

## Synthesis

The cyclam-tris(NTA) scaffold was synthesized similarly as described.<sup>19</sup> In the first step H-Glu(OBz)-OtBu hydrochloride (1) was treated with excess *t*-butyl bromoacetate (2) under basic

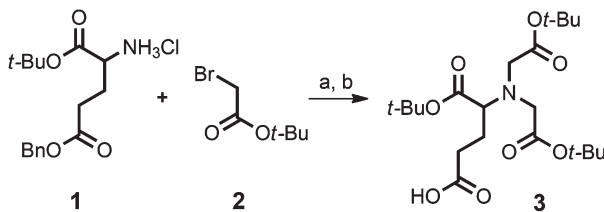


Fig. 4 Synthesis of the cyclam-tris(NTA)-propanoic acid (3). (a) DIEA, DMF, 55 °C, 12 h; 85%; (b) H<sub>2</sub>, Pd/C, MeOH; 74%.

conditions followed by benzyl ester cleavage *via* Pd-catalyzed hydrogenolysis to afford protected NTA-propanoic acid (3) in 63% yield over both steps (Fig. 4).

Next the cyclam platform (4) was equipped with three equivalents of tris(NTA)-propanoic acid (3) by standard peptide coupling (TBTU). TFA cleavage of the *t*-butyl esters and neutralization with sodium hydroxide afforded gave cyclam-tris(NTA) sodium salt (6) which was used as a reference in the ELISA binding experiments with IC16-scFv (Fig. 5). The free secondary amine of intermediate (5) was elongated with *N*-benzyloxy-carbonyl-6-aminohexanoic acid, followed by hydrogenolytic release of its primary amine to yield 7.<sup>20</sup>

Finally NTA-cyclam platform (7) was attached at the tip of its aminohexanoyl spacer to the PMB-protected aminopyrazole trimer (8) (HCTU/Cl-HOBt).<sup>13</sup> Simultaneous cleavage of all *t*-butyl

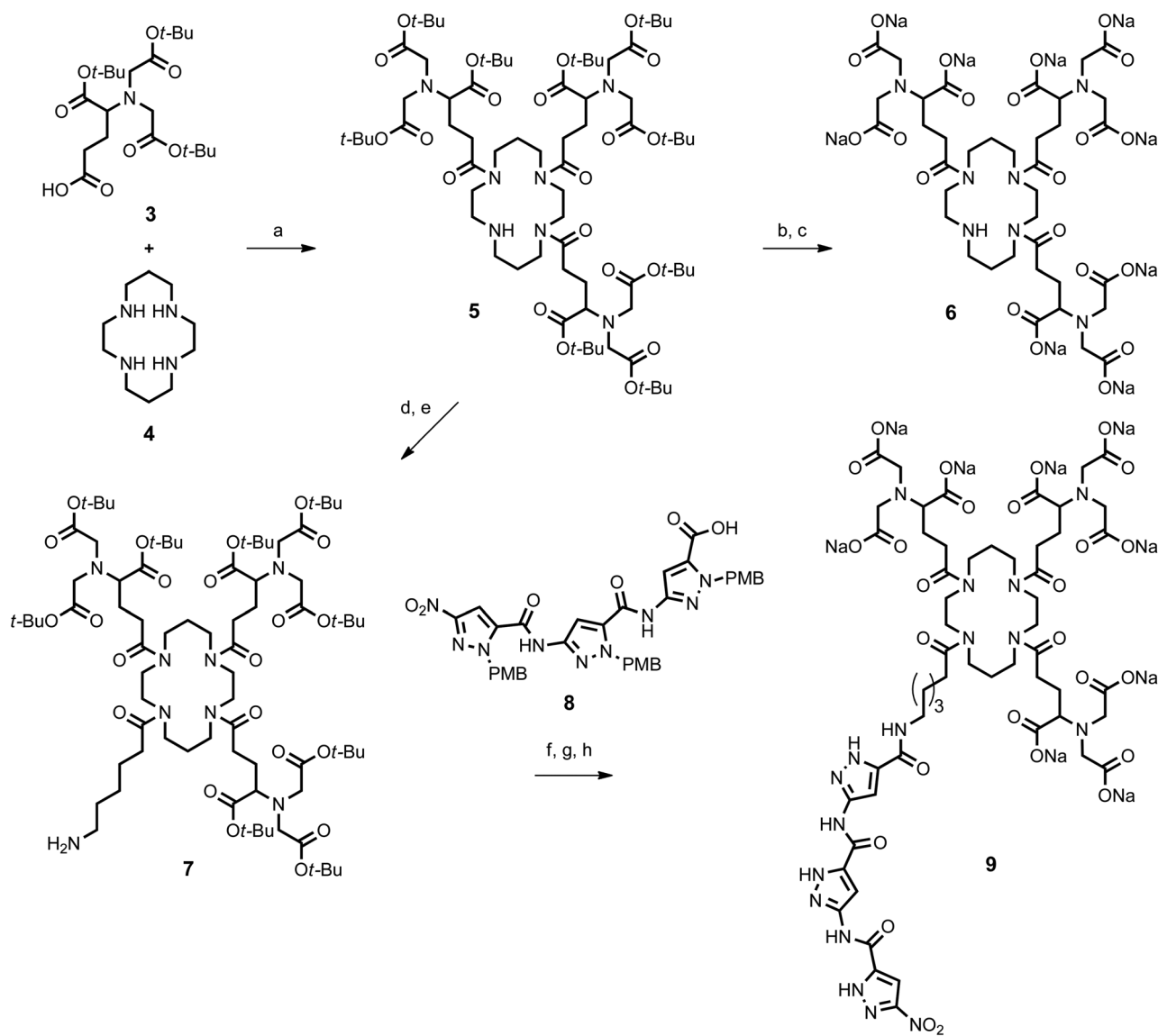


Fig. 5 Synthesis of cyclam-tris(NTA) sodium salt (6) and aminopyrazol-trimer-cyclam-tris(NTA) sodium salt (9). (a) TBTU, DIEA, CH<sub>2</sub>Cl<sub>2</sub>, rt, 24 h, 46%; (b) CH<sub>2</sub>Cl<sub>2</sub>/TFA 7:1, rt, 24 h, 88%; (c) 1 M NaOH, rt, 10 min, 99%; (d) Cbz-6-aminohexanoic acid, TBTU, DIEA, CH<sub>2</sub>Cl<sub>2</sub>, rt, 24 h, 85%; (e) H<sub>2</sub>, Pd/C, MeOH, 90%; (f) HCTU, Cl-HOBt, DIEA, CH<sub>2</sub>Cl<sub>2</sub>/DMF 2:1, 0 °C→rt, 48 h, 33%; (g) TFA, 70 °C, 5 h, 85%; (h) NaOH, Et<sub>2</sub>O, MeOH, 75%.



ester and PMB groups was effected in hot trifluoroacetic acid, and subsequent treatment with sodium hydroxide furnished the desired aminopyrazole-cyclam-tris(NTA) sodium salt (9).

### Complexation of IC16-scFv with AP-Ni-NTA-cyclam

**IC16-scFv.** The variable domains of the heavy ( $V_H$ ) and light chain ( $V_L$ ) of IC16 were cloned into pET22b allowing the periplasmic expression with C-terminal myc- and His<sub>6</sub>-tags in *E. coli*. IC16-scFv was purified *via* immobilized metal chelating chromatography (IMAC) and  $\text{A}\beta(1-16)$ -GB1 affinity purification (Fig. 6). Purified IC16-scFv binds to  $\text{A}\beta(2-8)$  with a  $K_d$  of 112 nM.<sup>18</sup>

Complex formation between the antibody and the aminopyrazole trimer was confirmed by native polyacrylamid electrophoresis (PAGE) (Fig. 7). The His<sub>6</sub>-IC16-scFv was incubated with increasing concentrations of the AP-tris(NTA)-cyclam (9), that had been associated with a 60-fold excess of  $\text{Ni}^{2+}$  ions. Successful binding of three negatively charged AP-tris(NTA)-cyclam molecules to IC16-scFv led to a pI-shift of the antibody from 5.9 to 5.4, thus changing the migration speed when separated on a native gel with a pH of 6.7. This was observed for all concentrations higher than a 30-fold excess of (9).

After verification of the complex formation we further investigated the binding properties of the self-assembled hybrid compound towards  $\text{A}\beta$  by use of enzyme-linked immunosorbent assays (ELISA).

In order to measure the affinity enhancement of the IC16-scFv induced by complex formation with the aminopyrazole-cyclam-tris(NTA) moiety we applied 120 nM IC16-scFv corresponding to approximately semimaximal binding (Fig. 8, top).

Addition of AP-tris(Ni-NTA)-cyclam Ni-(9) strongly enhanced the affinity of IC16-scFv to  $\text{A}\beta(1-42)$  in a dose-dependent manner, indicating the improved binding properties of the hybrid (Fig. 8, bottom). Already a two-fold excess (250 nM) of AP-tris(Ni-NTA)-cyclam led to increased 1.75-fold binding, whereas a 20-fold excess (2.5  $\mu\text{M}$ ) nearly doubled the antibody affinity to  $\text{A}\beta(1-42)$ . Finally, addition of a 160-fold excess (20  $\mu\text{M}$ ) of Ni-(9) raised  $\text{A}\beta(1-42)$  binding to 4-fold relative of the level of the antibody fragment alone.

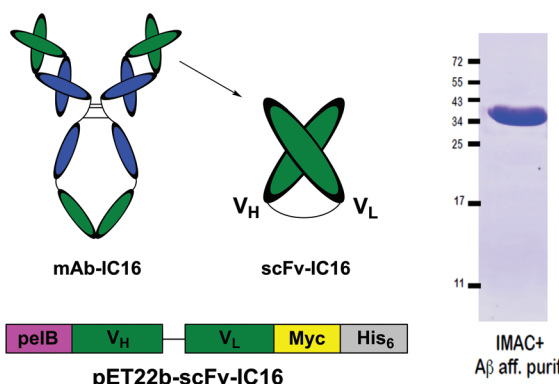


Fig. 6 Schematic representation of the His<sub>6</sub>-IC16-scFv preparation (left) and purity control after IMAC purification and  $\text{A}\beta$ -affinity polishing (right).

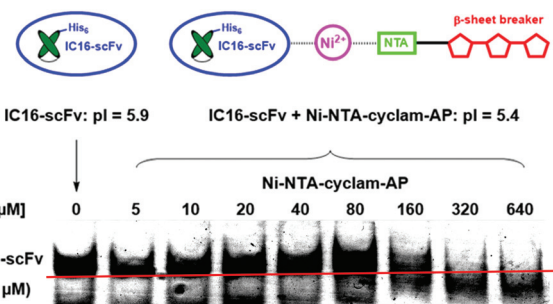


Fig. 7 Native PAGE for verification of complex formation between IC16-scFv (5  $\mu\text{M}$ ) and increasing amounts of Ni-NTA-cyclam-AP. Gel pH = 6.7.

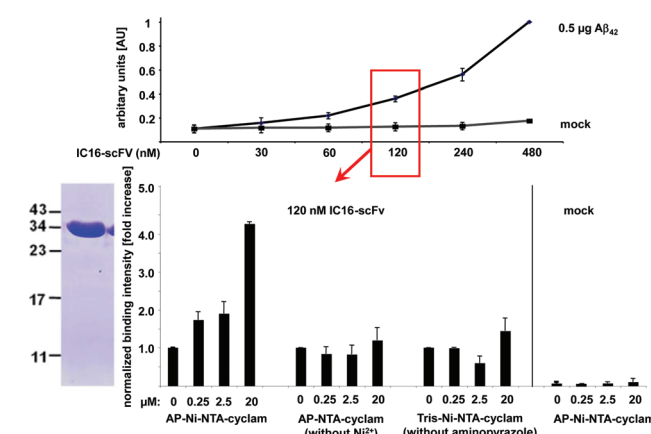


Fig. 8 ELISA-experiment for the investigation of binding properties of the self-assembled complex between AP-Ni-NTA-cyclam and IC16-scFv. Top: dose response chart of IC16-scFv binding to  $\text{A}\beta(1-42)$ . Bottom: 120 nM IC16-scFv was complexed with increasing amounts of either AP-Ni-NTA-cyclam, AP-NTA-cyclam or Tris-Ni-NTA-cyclam. Binding intensities are shown in comparison to 120 nM IC16-scFv alone ( $n$ -fold increase).

To verify that the affinity enhancement is related to complex formation between the IC16-scFv antibody fragment and AP-tris(Ni-NTA)-cyclam Ni-(9), the same experiment was carried out without  $\text{Ni}^{2+}$ -ions, thus preventing binding of AP-tris(Ni-NTA)-cyclam to the His-tag of IC16-scFv. Here, the binding of IC16-scFv was not influenced, indicating that hybrid formation is essential for affinity enhancement. In addition application of tris(NTA)-cyclam unit (6), which lacks the AP trimer, also did not affect the affinity of IC16-scFv to  $\text{A}\beta(1-42)$ , demonstrating the functional role of the AP moiety. In the absence of IC16-scFv we yielded no significant signals above background, confirming the lack of non-specific binding of the primary and secondary antibody used for the ELISA assay. We would like to emphasize that the two above-described negative control experiments strongly support the idea, that both parts of the self-assembled hybrid complex recognize different epitopes on the  $\text{A}\beta(1-42)$  target simultaneously, just as proposed in Fig. 2.

Altogether the ELISA data nicely reflect the results from native PAGE, because maximal binding occurred only when AP-trimer-tris(NTA)-cyclam Ni-(9) was added to IC16-scFv in concentrations higher than a 30-fold excess.

## Conclusion

In summary we demonstrated that the non-covalent  $\text{Ni}^{2+}$ -mediated hybridization of IC16-scFv with the AP-trimer-tris(NTA)-cyclam (9) strongly increased antibody affinity towards  $\text{A}\beta(1-42)$ . Various ELISA experiments with truncated versions of the self-assembled hybrid complex strongly suggest, that the specific binding properties of an antibody can be combined with the unspecific backbone recognition of a  $\beta$ -sheet binder and lead to significant affinity increase.

These results may open a promising new path for the development of enhanced antibodies applicable in amyloid diagnostics and possibly even in therapeutic applications to  $\text{A}\beta$ -related neurodegenerative disorders.

## Experimental

### Native polyacrylamid gel electrophoresis

Expression and purification of scFv-IC16 has been described before.<sup>18</sup> AP-trimer-tris(NTA)-cyclam Ni-(9) was complexed with  $\text{Ni}^{2+}$  with a 60-fold excess of  $\text{NiSO}_4$  for 30 min at rt. 5  $\mu\text{M}$  of purified IC16-scFv were incubated with increasing amounts of Ni-(9) for 30 min at rt. Fractions of 2  $\mu\text{g}$  of IC16-scFv were then diluted in native sample buffer (5% sucrose, 100 mM sodium phosphate, pH 6.7) and loaded on a phosphate buffered (pH 6.7) 10% polyacrylamid gel. After electrophoresis at 100 V for 1.5 h in native running buffer (100 mM sodium phosphate pH 6.7) the gel was stained with Coomassie blue.

### ELISA

Wells of a 96-well Maxisorp plate (Nunc, Thermo Scientific, Waltham, MA, USA) were coated with 500 ng of synthetic  $\text{A}\beta(1-42)$  (JPT, Berlin, Germany), that were diluted in 50 mM  $\text{NaHCO}_3$ , pH 8.3 over night at rt. Following washing with water, unspecific binding sites were blocked with PBS/5% skim milk for 2 h at rt. After removal of the blocking buffer increasing amounts of purified IC16-scFv, diluted in PBST/0.2% milk, were added to the wells and incubated for 2 h at rt. Subsequently, the wells were washed three times with PBS, 0.1% Tween-20 (PBS-T) and then probed for 1 h at rt with 9E10 anti-Myc mAb, that has been derived from hybridoma supernatant and diluted 1:2 in PBS-T. After three additional washing steps with PBS-T, the antibody complex was detected with an HRP-conjugated goat anti-mouse-IgG (Pierce, Thermo Scientific, Waltham, MA, USA; 1:5000 diluted in PBS-T). Signals were quantified by using the OptEIA detections reagent (BD Bioscience, Franklin Lakes, NJ, USA) according to the manufacturer's recommendations.

In order to determine an increased affinity of IC16-scFv in complex with AP-trimer-tris(NTA)-cyclam Ni-(9), 120 nM of IC16-scFv were preincubated in PBST/0.2% milk for 30 min

with variable concentrations of Ni-(9) (60-fold molar excess of  $\text{Ni}^{2+}$ ). As controls IC16-scFv was either incubated with (9) in the absence of  $\text{Ni}^{2+}$  ions or with Tris(NTA)-cyclam Ni-(6) that lacks the AP.

### Synthesis

**General procedures.** Unless otherwise noted, materials and reagents were obtained from commercial suppliers and were used without further purification. Cyclohexane and ethyl acetate were freshly distilled before use. Air- and moisture-sensitive reactions were performed under an argon atmosphere. Silica gel (Kieselgel 60, Merck) was used for column chromatography. TLC was performed on *Macherey-Nagel* ALUGRAM and POLYGRAM SIL G/UV254, 0.2 mm thick.

$^1\text{H}$  NMR measurements were recorded on a Bruker Advance DRX500 spectrometer. Chemical shifts are reported in parts per million (ppm) and were referenced to  $\text{CDCl}_3$  ( $\delta$  H7.25),  $\text{DMSO-d}_6$  ( $\delta$  H2.50) and  $\text{D}_2\text{O}$  ( $\delta$  H4.80). NMR assignments were made using a 1D technique. Multiplicities are described using the following abbreviations: s = singlet, d = doublet, t = triplet, q = quartet; quint = quintet; sext = sextet; m = multiplet, br = broad. High-resolution mass spectra (HRMS) were recorded with a *Bruker* *maxis 4G* time of flight mass spectrometer in positive or negative ion electrospray mode.

*2,2',2'',2'',2''',2''''-(((1,4,8,11-Tetraazacyclotetradecane-1,4,8-triyl)-tris(1-carboxy-4-oxobutane-4,1-diyl))tris(azantriyl))hexa-acetic acid (5a).* 0.359 g Tris(tbutyl-NTA)cyclam (5) (0.25 mmol, 1.0 eq.) was dissolved in 2 mL TFA and 14 mL dichloromethane and stirred for 24 h at rt. The solvent was evaporated under reduced pressure and the residue was redissolved in TFA. Cold diethyl ether was added to the solution, the precipitating solid was centrifuged and washed three times with cold diethyl ether. The solid was dried *in vacuo* to afford 0.203 g (0.22 mmol, 91%) of (5a) as a pale yellow solid. The product was directly used to form the sodium salt.

*2,2',2'',2'',2''',2''''-(((1,4,8,11-Tetraazacyclo-tetradecane-1,4,8-triyl)-tris(1-carboxylat-4-oxobutane-4,1-diyl))tris(azantriyl))-hexaacetate nona sodium salt (6).* 0.050 g Tris(NTA)cyclam (5a) (0.053 mmol, 1.0 eq.) was dissolved in 0.481 mL 1 M NaOH (0.481 mmol, 9.0 eq.) and stirred for 10 min at rt. Subsequently the solution was lyophilized and furnished 0.060 g (0.053 mmol, 99%) of (6) as a pale yellow solid.  $^1\text{H}$  NMR (500 MHz,  $\text{D}_2\text{O}$ ):  $\delta$  [ppm] = 1.85–2.01 (m, 10H, H-4, H-8, H-13), 2.46–2.48 (m, 6H, H-7, H-9, H-12), 2.75 (m, 2H, H-14), 2.82–2.87 (m, 2H, H-15), 3.11–3.28 (m, 15H, H-2, H-3), 3.48–3.58 (m, 13H, H-5, H-10, H-11, H-16, H-17).

*Hexa-tert-butyl-2,2',2'',2'',2''''-(((11-(6-(3-(3-nitro-1H-pyrazol-5-carboxamido)-1H-pyrazol-5-carboxamido)-1H-pyra-zol-5-carboxamido)hexanoyl)-1,4,8,11-tetraazacyclotetradecane-1,4,8-triyl)tris(1-(tert-butoxy)-1,5-dioxo-pentane-5,2-diyl))tris(azantriyl)) hexaacetate (9a).* Under argon 0.043 g PMB-protected trimer carboxylic acid (8) (0.06 mmol, 1.0 eq.) was dissolved in 10 mL dry dichloromethane and 5 mL dry DMF. 0.029 g HCTU (0.07 mmol, 1.2 eq.), 0.025 g Cl-HOBt (0.15 mmol, 2.5 eq.) and 0.04 mL DIEA (0.23 mol, 4.0 eq.) were added to the solution, cooled down to 0 °C and stirred for additional 10 min. Sub-



sequently, 0.136 g of *t*-butyl ester-protected amine (7) (0.09 mmol, 1.5 eq.) was added to the reaction mixture and stirred for 48 h at rt. The solvent was removed and the residue was dissolved in ethyl acetate. The organic layer was washed three times with saturated aqueous NaHCO<sub>3</sub> as well as three times with saturated aqueous NaCl, dried over magnesium sulfate and evaporated under reduced pressure. The crude product was purified by column chromatography (ethyl acetate) and gave 0.043 g (0.02 mmol, 33%) of (9a) as a colorless solid. R<sub>F</sub>: 0.44 (ethyl acetate). <sup>1</sup>H-NMR (500 MHz, DMSO-d<sub>6</sub>): δ [ppm] = 1.24–1.31 (m, 2H), 1.38 (s, 54H, H-1), 1.40 (s, 27H, H-1'), 1.50–1.52 (m, 8H), 1.65–1.84 (m, 11H), 2.34–2.46 (m, 8H), 3.36–3.40 (m, 27H), 3.33–3.36 (m, 27H), 3.70–3.71 (3 s, 9H, H-35), 5.61 (s, 2H, H-30), 5.67 (s, 2H, H-30), 5.81 (s, 2H, H-30), 6.85–6.91 (m, 7H, H-28, H-32, H-33), 7.16–7.30 (m, 7H, H-32, H-33), 7.71 (s, 1H, H-28), 7.98 (s, 2H, H-28), 8.62 (bs, 1H, H-25), 11.33 (s, 1H, H-36), 11.49 (s, 1H, H-36). HRMS (ESI<sup>†</sup>): for C<sub>115</sub>H<sub>171</sub>N<sub>17</sub>O<sub>30</sub>Na: calcd: 2294.2301, found: 2294.2476, for C<sub>115</sub>H<sub>171</sub>N<sub>17</sub>O<sub>30</sub>Na<sub>2</sub>: calcd: 1158.6097, found: 1158.6217.

2,2',2'',2'',2'''-(((11-(6-(3-(3-Nitro-1*H*-pyrazol-5-carboxamido)-1*H*-pyrazol-5-carboxamido)-1*H*-pyrazol-5-carboxamido)-hexanoyl)-1,4,8,11-tetraazacyclotetradecane-1,4,8-triyl)tris(1-carboxy-4-oxobutane-4,1-diyl))tris(azantriyl)hexaacetic acid (9b). Under argon 0.028 g (0.01 mmol, 1.0 eq.) trimer-tris(*t*Bu-NTA)cyclam (9a) was dissolved in 4 mL dry TFA and stirred for 5 h at 70 °C in a closed system. Cold diethyl ether was added to the cooled reaction mixture; the precipitating solid was centrifuged and washed three times with cold diethyl ether. The crude product was dried *in vacuo* to afford 0.019 g (0.01 mmol, 99%) of (9b) as a colorless solid, which was directly converted into the sodium salt.

2,2',2'',2'',2'''-(((11-(6-(3-(3-Nitro-1*H*-pyrazol-5-carboxamido)-1*H*-pyrazol-5-carboxamido)-1*H*-pyrazol-5-carboxamido)-hexanoyl)-1,4,8,11-tetraazacyclotetradecane-1,4,8-triyl)tris(1-carboxylat-4-oxobutane-4,1-diyl))tris(azantriyl) hexaacetic acid nona sodium salt (9). 5.0 mg of the deprotected hybrid compound (9b) (0.004 mmol, 1.0 eq.) was dissolved in 1 mL 2 M NaOH, and 2 mL diethyl ether were added to the solution. After drop-wise addition of methanol (up to 1 mL) a yellow solid precipitated. The solution was centrifuged and the solid was washed with cold diethyl ether. Redissolution in water and subsequent lyophilization gave 5.2 mg (0.003 mmol, 75%) of (9) as a pale yellow solid. <sup>1</sup>H-NMR (500 MHz, D<sub>2</sub>O): δ [ppm] = 1.44 (m, 2H, H-19), 1.66 (m, 4H, H-18, H-20), 1.86–2.00 (m, 10H, H-4, H-8, H-13), 2.45 (m, 8H, H-5, H-17), 3.12–3.63 (m, 33H, H-2, H-3, H-7, H-9, H-10, H-11, H-12, H-14, H-15, H-16, H-21), 6.81 (s, 1H, H-25), 6.93 (s, 1H, H-25), 7.46 (s, 1H, H-25). HPLC: 92–99% (retention time: 2.1–3.0 min, RP 18 column, 214 nm detection, flow rate: 1.0 mL min<sup>-1</sup>, linear gradient 95–40% eluent A in 30 min, eluent A: 0.1% TFA in water, eluent B: acetonitrile).

## Acknowledgements

M. Hellmert thanks the Bruno-Werdelmann foundation for financial support. A. Müller-Schiffmann received a grant from

the Forschungskommission of the University of Düsseldorf Medical School.

## Notes and references

- 1 J. Hardy and D. J. Selkoe, *Science*, 2002, **297**, 353–356.
- 2 I. W. Hamley, *Chem. Rev.*, 2012, **112**, 5147–5192.
- 3 J. M. Nussbaum, M. E. Seward and G. S. Bloom, *Prion*, 2013, **7**, 14–19.
- 4 K. R. Patterson, C. Remmers, Y. Fu, S. Brooker, N. M. Kanaan, L. Vana, S. Ward, J. F. Reyes, K. Philibert, M. J. Glucksman and L. I. Binder, *J. Biol. Chem.*, 2011, **286**, 23063–23076.
- 5 C. Haass and D. Selkoe, *Nat. Rev. Mol. Cell Biol.*, 2007, **8**, 101–112.
- 6 I. Kim, J. Lee, H. J. Hong, E. S. Jung, Y. H. Ku, I. K. Jeong, Y. M. Cho, I. So, K. S. Park and I. Mook-Jung, *J. Alzheimer's Dis.*, 2010, **19**, 1371–1376.
- 7 E. Head and I. T. Lott, *Curr. Opin. Neurobiol.*, 2004, **17**, 95–100.
- 8 B. L. Kagan, *Biophys. J.*, 2011, **100**, 1597–1598.
- 9 S. J. Soscia, J. E. Kirby, K. J. Washicosky, S. M. Tucker, M. Ingelsson, B. Hyman, M. A. Burton, L. E. Goldstein, S. Duong, R. E. Tanzi and R. D. Moir, *PLoS One*, 2010, **5**, e9505.
- 10 G. Bitan, S. S. Vollers and D. B. Teplow, *J. Biol. Chem.*, 2003, **278**, 34882–34889.
- 11 T. Schrader and C. Kirsten, *Chem. Commun.*, 1996, 2089–2090.
- 12 C. N. Kirsten and T. H. Schrader, *J. Am. Chem. Soc.*, 1997, **119**, 12061–12068.
- 13 P. Rzepecki, M. Wehner, O. Molt, R. Zadmard, K. Harms and T. Schrader, *Synthesis*, 2003, 1815–1826.
- 14 K. Hochdörffer, J. März-Berberich, L. Nagel-Steiger, M. Epple, W. Meyer-Zaika, A. H. C. Horn, H. Sticht, S. Sinha, G. Bitan and T. Schrader, *J. Am. Chem. Soc.*, 2011, **133**, 4348–4358.
- 15 A. Müller-Schiffmann, J. März-Berberich, A. Andreyeva, R. Röncke, D. Bartnik, O. Brener, J. Kutzsche, A. H. C. Horn, M. Hellmert, J. Polkowska, K. Gottmann, K. G. Reymann, S. A. Funke, L. Nagel-Steiger, C. Moriscot, G. Schoehn, H. Sticht, D. Willbold, T. Schrader and C. Korth, *Angew. Chem., Int. Ed.*, 2010, **49**, 8743–8746.
- 16 K. Lobello, J. M. Ryan, E. Liu, G. Rippon and R. Black, *Int. J. Alzheimer's Dis.*, 2012, 628070.
- 17 Y.-J. Wang, *Nat. Rev.*, 2014, **10**, 188–189.
- 18 S. Dornieden, A. Müller-Schiffmann, H. Sticht, N. Jiang, Y. Cinar, M. Wördehoff, C. Korth, S. Aileen Funke and D. Willbold, *PLoS One*, 2013, **8**, e59820.
- 19 S. Lata, A. Reichel, R. Brock, R. Tampé and J. Piehler, *J. Am. Chem. Soc.*, 2005, **127**, 10205–10215.
- 20 J. T. Heeres, S.-H. Kim, B. J. Leslie, E. A. Lidstone, B. T. Cunningham and P. J. Hergenrother, *J. Am. Chem. Soc.*, 2009, **131**, 18202–18203.

